Energy distribution in the near-threshold electron-impact ionization of atoms and ions

P. V. Grujić
Institute of Physics, P. O. Box 57, 11001 Belgrade, Yugoslavia
(Received 27 December 1983)

A concise overview of the present situation of the near-threshold energy distribution investigations for electron-atom (-ion) ionizing collisions is given. By making use of an essentially perturbative approach, the distribution function has been calculated for two extreme regimes of the two-electron final state: (i) $\epsilon_1 \approx \epsilon_2$ and (ii) $\epsilon_{1,2} \ll \epsilon_{2,1}$, where $\epsilon_{1,2}$ are the escaping-electron final energies. It is shown that within the classical Wannier theory (linear configuration) one obtains the flat distribution function in both cases. The calculations for case (ii) are compared with recent Coulomb-dipole results. A brief discussion of some conceptual differences between Wannier and Coulomb-dipole theories is also given.

I. INTRODUCTION

Near-threshold phenomena continue to attract much attention of both experimentalists and theoreticians and the overall activity on that subject appears in the state of a rapid expansion. After the early studies of the energy dependence of various multiple escape processes above the breakup thresholds, which have provided values of the exponent in the corresponding threshold laws

$$\sigma_{\text{ion}} = \text{const} \times E^{\kappa} , \tag{1.1}$$

where E is the total energy of the system, the interest has been widened to comprise other phenomena, like the energy, mutual angle and angular momenta distributions and their energy dependence.[1] Despite a great progress made up to now and many more or less firmly established results, a number of unsettled questions still persist, even at the conceptual level. One of the controversial issues on that matter appears to be the very model used to describe the way a multiple escape takes place. Two principal assumptions have emerged up to now. (i) Wannier's model[2] which takes a complete dynamical symmetry of the final configuration as a starting point. (ii) Temkin's approach,[3] based on the asymmetrical, Coulomb-dipole final-state interaction. The latter predicts an analytical expression for the ionization threshold law,[4] which differs from the simple power law of Eq. (1.1). However, it turns out that a noticeable difference between predicted threshold behavior appears presumably so close to the threshold that the experiments can provide a clear evidence in favor of either of approaches mentioned above,[5] though the measurement corroborates marginally better Wannier theory. Hence, apart from importance of their own, it is of interest to examine other measurable quantities, which can distinguish between two approaches. In the present study, we examine analytically the final energy partition between outgoing electrons, within the classical Wannier theory, adopting in part the method due to Vinkalns and Gailitis,[6] already successfully extended and applied in the study of a number of ionizational processes.[7] As the distribution of final energy has been the subject of both numerical and experimental studies, we first quote some of the results obtained up to now.

The first attempt to derive numerically energy distribution within the classical model (linear configuration)[6] provided deviation from the uniform partition by less than 1% for a neutral target ($Z=1$). It should be noted that these computations relied heavily on the quasiergodic hypothesis,[2] confining the calculations to the final states only. This assumption has been removed in the subsequent classical trajectory calculations,[8] but the latter still pertained to Wannier theory, via the assumption of the one-dimensional phase-space volume behavior. Computations provided results confirming the earlier (restricted) numerical findings, at least for $Z=1,2$, (see Fig. 3 of Ref. 8). For $Z>2$, one may argue that a deviation from strict uniformity may show up (see Fig. 7 of Ref. 8 and discussion there). It should be noted, however, that all these computations were not a proper Monte Carlo calculation (or, equivalently, simulations of experimental measurements), and the most they can yield is a proof of an actual uniform distribution (or, possibly, some other highly specific distribution, like δ function). All computations, also, have been carried out for the plane configurations ($L=0,1$). All these restrictions, except the last one, have been removed in the very recent calculations by Read,[9] who has repeated Vinkalns-Gailitis computations with full statistics of Wannier diverging orbits.[2] The energy distribution for the plane motion thus obtained, exhibits a shallow convex shape, with wings surpressed by about 5% of the maximum at the centers ($\epsilon_1 \approx \epsilon_2$). It is interesting to note that the derivative of the distribution function becomes very large (in magnitude) at the very wings (ϵ_1, $\epsilon_2 \approx 0$), Fig. 3 of Ref. 9. One encounters a similar situation in the case of positron-atom near-threshold ionization, when a sudden collapse of the distribution function occurs at $\epsilon(\text{positron}) \approx 7/20E$ (see inset in Fig. 3 in the second reference quoted under Ref. 8). We emphasize here, that this cutoff *does not* depend on the ion mass (unlike the threshold law, derived in the same paper) and appears for $e^+ + \text{H}$ system as well.

(Semi) quantum-mechanical calculations did not pay particular attention to the energy distribution, but one can infer the latter from the general results. Thus Rau[10] deduced from his Wannier-type quantum-mechanical calculations that the distribution should be a broad Gaussian correction superimposed upon otherwise flat distribution. In his semiclassical study[11] Klar was able to deduce the uniform distribution only at $\epsilon_1 \approx \epsilon_2 \approx E/2$. (See also recent work by Feagin,[12] for a general discussion of previous nonclassical calculations.) In this context mention should be made also of the combined analytical-numerical calculations by Peterkop and Liepinsh,[13] who derived also uniform distribution within the semiclassical Wannier theory. We mention finally calculations by Yurev,[14] who obtains for a double photoionization ($L=1$), within his quantum-mechanical perturbative method, almost uniform partition, with a shallow minimum, which becomes more pronounced as the total energy increases. In comparing his results with those by Read[9] (with maxima rather than minima), we note first that the former are obtained for different angular momentum ($L=1$), and second that they yield the threshold exponent κ in Eq. (1.1) 1.13 rather than 1.056 ($Z=2$).[2]

As for the experimental evidence, we mention only two important features (the reader may consult Ref. 9 for a more detailed overview) which have emerged from almost all measurements: (a) a flat distribution within the energy range $E/5 \lesssim \epsilon_{1,2} \lesssim 4/5E$, with wings undetermined, (b) this distribution persists up to an energy which is above that which delimits Wannier threshold behavior. Findings by Bottcher,[15] who solved the corresponding Schrödinger time-dependent equation numerically (within linear configuration), appear consistent with these experimental data. We notice that points (a) and (b), taken together, imply that the problem of the cross section threshold behavior and energy partition function are not necessarily crucially interdependent.

We now turn to the latest Temkin's results,[4] obtained via the Coulomb-dipole theory (for the previous energy distribution see Ref. 3). One observes immediately two striking features at the close inspection of Fig. 2 of Ref. 3: (i) an oscillatory behavior of the distribution in the range $\epsilon_{1,2} < E/5$, (ii) a sharp descent to zero at $\epsilon_{1,2} \ll E/2$ (actually, this feature is not conspicuous in the figure, but is pointed out in the text). Now, if one averages over oscillations, it turns out that the overall picture is not inconsistent with the latest numerical findings,[9] discussed above.

Whether wing oscillations would be smeared out by inclusion of higher angular momentum terms[3] is yet to be settled. We merely note there that undulatory structures pertain to monopole-dipole interaction, both within the classical[16] and quantum-mechanical[17] pictures.

Our aim in the present work is to investigate the possibility of deriving the energy distribution within the classical dynamics model. Such an attempt has been already made,[18] making use of Vinkalns-Gailitis (VG) approach, but cannot be regarded fully satisfactory, for the following reasons. The linearized, approximate (VG) solution is valid only within a (small) part of the Wannier Coulomb zone (our SCZ in Fig. 1). While knowledge of the relevant

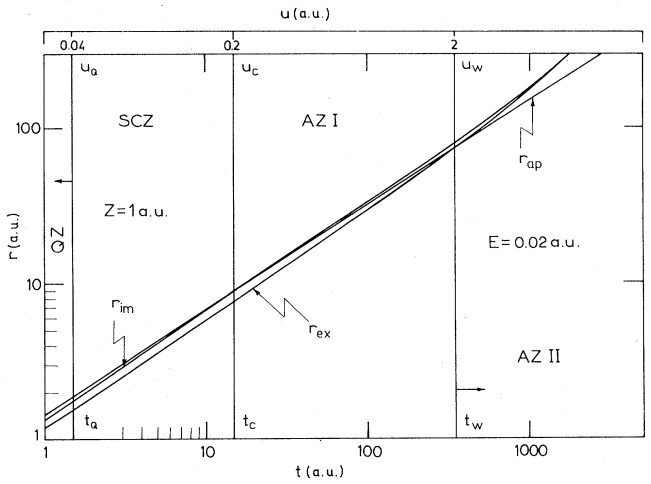

FIG. 1. The exact solution of Eq. (2.9) is r_{ex} [Eq. (2.10)], approximate solution (2.13) is r_{ap}, and the improved approximate solution [Eqs. (2.15) and (2.16)] is r_{im}, vs time, for $Z=1$ a.u. and $E=0.02$ a.u. Value for t_A (see text) in this particular case assumes 6147 a.u. and is not comprised by the figure. Note the scale for u variable [Eq. (2.11)], on which numerical values for u_Q, u_C, u_W, and u_A (not shown) are independent of Z and E. The quantum-mechanical zone (QZ) extends up to zero.

deviation from the so-called leading configuration[7] is sufficient to determine the threshold law, it does not contain enough information for deducing other observables, like various distribution functions. One has, therefore, to carry out calculations throughout the intermediate region of the configuration space, so as to carry over initial information to the free zone (where measurements are made). In fact, Wannier[2] did it in the sense that he was able to show that the Coulomb-zone solution does correspond to a second-asymptotic-zone equation of motion, with a structure equally suitable for deriving the threshold law. However, to derive a distribution function, one needs a precise (quantitative) relation between the initial conditions (at the reaction zone boundary) and the parameters appearing in the final-state solution. As we shall see, we have succeeded in obtaining such solutions only in a restricted part of the phase space.[13]

In Sec. II, which is of a preliminary character, we first demonstrate the uniqueness of the Wannier saddle point and then partition the configuration space into a number of convenient zones. Derivation of the energy distribution for two cases: (i) $\epsilon_1 \approx \epsilon_2$, (ii) $\epsilon_{1,2} \ll \epsilon_{2,1}$ is presented in Sec. III. In the last section we make some general remarks (IV A) and finally conclude with a brief discussion of what appears to be a conceptual difference between Coulomb-dipole and Coulomb-Coulomb types of final-states interaction near the ionization threshold (IV B). In case (i) the VG method has been adopted as a starting point, whereas regime (ii) we investigate via a monopole-(dynamical) dipole interaction model, which may be viewed as a counterpart of the latest version of Coulomb-dipole quantum theory.[4]

II. DOUBLE-ESCAPE FINAL CONFIGURATIONS

A. Wannier potential ridge

Here we show that for the case of two identical particle escape above the threshold Wannier saddle point: $r_1=r_2$, $\theta_{12}=\pi$, is a unique configuration around which an ionization can proceed. We treat a simplified case:[6] $\theta_{12}=\pi$, but it can be easily shown that the argument loses nothing of its generality for sufficiently small total energy E.

Let two electrons recede from the residual ion of charge Z (atomic units are used throughout), along a common straight line, with distances from the ion (situated at the origin): r_1, r_2. Corresponding Newton's equations are

$$\frac{d^2r_i}{dt^2}=\frac{-Z}{r_i^2}+\frac{1}{(r_1+r_2)^2},\quad i=1,2\ . \tag{2.1}$$

Now, in searching for a stationary solution (no energy exchange between electrons), we put

$$r_2=\beta r_1 \tag{2.2}$$

(with β a real constant). With this correlation constraint, Eqs. (2.1) become (formally) single-particle equations

$$\frac{d^2r_i}{dt^2}=\frac{Z_i}{r_i^2},\quad i=1,2 \tag{2.3}$$

$$Z_1=Z-\frac{1}{(1+\beta)^2}\ , \tag{2.4}$$

$$Z_2=Z-\frac{1}{\left[1+\frac{1}{\beta}\right]^2}\ . \tag{2.5}$$

Equations (2.3) possess the first integrals ϵ_1 and ϵ_2 satisfying the following equation:

$$\frac{dE}{dt}=\frac{d}{dt}(\epsilon_1+\epsilon_2)=(1+\beta^2)\frac{d^2r_1}{dt^2}-\left[\frac{Z_2}{\beta}-Z_1\right]\frac{1}{r_1^2}\ . \tag{2.6}$$

As can be seen by direct inspection, the energy E is conserved if and only if the correlation parameter is

$$\beta=1 \tag{2.7}$$

(Wannier ridge) which provides a completely symmetrical configuration

$$\vec{r}_1=-\vec{r}_2,\ Z_1=Z_2=Z-\frac{1}{4}\equiv\zeta\ . \tag{2.8}$$

B. Symmetrical escape zones

Before proceeding with further calculations, it is convenient to divide the configuration space around the ion into a number of zones. The criterion for separating r-variable space into distinct regions is partly physical and partly because of mathematical convenience, as we shall see below.[19] We first write Eqs. (2.1) in the form (without subscript)

$$\frac{d^2r}{dt^2}=-\frac{\zeta}{r^2} \tag{2.9}$$

which has the solution[6]

$$\sqrt{u(u+1)}-\tfrac{1}{2}\ln[2\sqrt{u(u+1)}+2u+1]-\frac{E^{3/2}2^{1/2}}{\zeta}t=0\ , \tag{2.10}$$

$$u\equiv Er/\zeta \tag{2.11}$$

with the usual convention $r(0)=0$. For further analysis it is convenient to distinguish the following zones in u-variable space: see Fig. 1, where corresponding values of r variable are given as well, for $Z=1$ a.u. and (typical) total energy $E=0.02$ a.u.

1. *Reaction zone (RZ): $u<0.04$*

It is the space within the sphere of radius r_Q, the latter being of the order of dimensions of the target in its initial state.[20] Value of r_Q is arbitrarily chosen to be of the order of 1 a_0, but we note that in actual calculations care must be taken that at specific E, r_Q is not too close (or even exceeds) to the next important point r_C, to be defined immediately. The main feature of the motion within RZ (and this is a crucial assumption of the Wannier model) is that it must be very complicated (both within the classical and quantum-mechanical pictures), that it is close to chaotic behavior (quasiergodic hypothesis). In other words, reaction zone serves here as a kind of black box and it is only outside the RZ that the symmetric motion makes sense.

2. *Strong correlation zone (SCZ)*

In the range

$$u_Q<u<u_C\equiv 0.2\text{ a.u.} \tag{2.12}$$

Equation (2.10) can be solved for u (see Ref. 6)

$$u^3\approx\frac{9E^3}{2\zeta^2}t^2\ . \tag{2.13}$$

It is to be noted that despite the explicit appearance of E in Eq. (2.13), motion is essentially independent of the energy in this region. [In fact, the solution (2.13) can be obtained directly from Eq. (2.9) for $E=0$].[7]

3. *First asymptotic zone (AZ I)*

Upper boundary of this zone is determined by the so-called Wannier point u_W

$$u_C<u<u_W\equiv 2\text{ a.u.}\ , \tag{2.14}$$

where correlations are supposed to cease. Here it is not possible to extract an explicit dependence of u on t, but an approximate solution can be found in the following way. We write [accounting for Eq. (2.13)]

$$r=\left[\frac{9}{2}\zeta\right]^{1/3}t^{2/3}+\delta\equiv r^{(0)}(t)+\delta(t) \tag{2.15}$$

with δ as a small perturbation of the symmetric case. Substituting Eq. (2.15) into Eq. (2.9), we have, within the linear approximation with respect to $\delta/r^{(0)}$

$$\delta=C_3t^{4/3}+C_4t^{-1/3}\ , \tag{2.16}$$

where C_3 and C_4 are arbitrary constants. If we define via Eq. (2.10)

$$t_C\equiv t(u=0.2)=0.056\,39\zeta E^{-3/2} \tag{2.17}$$

then by matching solution (2.16) at $t=t_C$, one has

$$C_4=-t_C^{5/3}C_3\ . \tag{2.18}$$

Additional relation between C_3 and C_4 is provided by matching the solution (2.15) with that in the second asymptotic region,[21] to be determined immediately.

4. *Second asymptotic zone (AZ II)*

It starts at $u_W(=2)$, with the corresponding "Wannier instant"

$$t_W=t(u=2)=1.303\,27\zeta E^{-3/2} \tag{2.19}$$

and ends at

$$t_F=t(u=25)=23.1827\zeta E^{-3/2} \tag{2.20}$$

after which the moment motion is essentially free. In between we may regard electrons to move almost freely (quasifree zone)

$$u-\frac{1}{2}\ln(4u)+\frac{1}{2}-\frac{1}{4u}-\frac{1}{\zeta}E^{3/2}\sqrt{2}t=0\ . \tag{2.21}$$

Now, matching solution (2.15) with (2.21) at $t=t_W$ we obtain

$$C_4=-1.2246\times10^{-3}\zeta^{4/3}E^{-3/2} \tag{2.22}$$

so that with Eq. (2.18) δ function from Eq. (2.16) is completely determined.

5. *Free zone (FZ)*

For nonzero energy we have a free-particle motion

$$r\approx\sqrt{E}t\ . \tag{2.23}$$

In the limit, $E\to0$, however, $t_W\to\infty$ and Eq. (2.13) [or Eq. (2.15)] covers entirely the configuration space available. This is the well-known property of the Coulomb force, that at zero energy particles follow parabolic trajectories, without asymptote (long-range force).

In Fig. 1 time intervals corresponding to various r zones are shown for $Z=1$, $E=0.02$ a.u., together with the exact solution [Eq. (2.10)], approximate one [Eq. (2.13)] and the improved approximation, Eqs. (2.15) and (2.16). As can be seen in Fig. 1, the improved solution not only better represents motion in its proper AZ I, but is closer to the exact one in SCZ, compared with the solution (2.13), the latter being a straight line in our log-log scale. Note, also, that at $t=t_W$ the improved solution possesses both the magnitude and its derivative closer to the exact one, than the simple Eq. (2.13).

III. THE ENERGY DISTRIBUTION

A. Motion in SCZ

The strong correlation means that the outgoing particles must follow trajectories that lie close to the saddle point: $r_1=r_2$, $\theta_{12}=\pi$ (motion along the potential ridge). One may, therefore, write[6]

$$r_{1,2}=r\pm\Delta,\quad 0\le\Delta\ll r\ . \tag{3.1}$$

Substituting this into Eqs. (2.1) we have

$$\frac{d^2\Delta}{dt^2}=Z\left[\frac{E}{\zeta}\right]^3\frac{\Delta}{u^3}\left[2\left[\frac{E}{\zeta}\right]\left[\frac{\Delta}{u}\right]+\cdots\right] \tag{3.2}$$

with u given by Eq. (2.13). Further, because of the condition in Eq. (3.1) imposed on the magnitude of the longitudinal deviation Δ, one may neglect linear (and higher) term(s) in the large square bracket of the right-hand side of Eq. (3.2), which yields the solution[6]

$$\Delta=C_1r^{\mu_1}+C_2r^{\mu_2}\ , \tag{3.3}$$

$$\mu_{1,2}=\frac{3}{4}\mp\frac{1}{8}\left[\frac{100Z-9}{\zeta}\right]^{1/2},\quad Z\ge1\ . \tag{3.4}$$

The first term describes the solution when electrons cross the boundary separating QZ from SCZ at different moments, but with such velocities that $r_1(t)\to r_2(t)$, $t\to\infty$. On the contrary, the second term corresponds to the case of simultaneous passing from QZ to SCZ, but with different velocities, so that Δ/r grows in time. If at $r=r_Q$ ($u=u_Q$, see Fig. 1) Δ/r is large enough, it will prevent both particles from escape and the slower electron will be recaptured by the residual ion. This difference depends on the magnitude of the (arbitrary) constant C_2, at a particular value of the energy E and there must exist such maximum value

$$C_2=C_2^{\max}(E) \tag{3.5}$$

that for $C_2>C_2^{\max}$ no ionization takes place. This limiting C_2 value is therefore proportional to the single-ionization probability. Further, as inferred from Eq. (3.3), under the (homothetic) scaling, arbitrary constants depend on the energy E as follows

$$C_1\sim E^{\mu_1-1},\ C_2\sim E^{\mu_2-1} \tag{3.6}$$

so that, according to Eq. (3.5) one has[6]

$$\sigma_{\text{ion}}\sim E^{\mu_2-1} \tag{3.7}$$

provided that distribution of C_2 *has no singular points* (quasiergodic hypothesis).[2] The latter assumption is crucial for the above derivation and has been criticized[3,4] as unfounded. We shall, however, postpone the discussion of this point to Sec. IV.

Now, for a particular choice of C_2, final energies of escaping particles are

$$\epsilon_{1,2}=\frac{1}{2}\dot{r}_{1,2}^2(C_2,t\to\infty)\ , \tag{3.8}$$

and the energy distribution is then obtained by[6]

$$F(\epsilon_{1,2})=\frac{dC_2}{d\epsilon_{1,2}} . \tag{3.9}$$

We need, therefore, (in principle) equation of motion in FZ, which implies a complete description of motion through all intermediate zones (see Fig. 1). On the other hand, Eq. (2.1) describes the three-body problem (though a somewhat restricted one), which is beyond the reach of our mathematical methods at present. We must therefore confine ourselves to those parts of the final states phase space where at least approximate solutions in the intermediate zones are possible. We find two such cases: (a) the quasisymmetrical configuration ($\epsilon_1 \approx \epsilon_2$), (b) extreme asymmetrical configuration ($\epsilon_1 \ll \epsilon_2$, or vice versa). We treat first case (a). Before proceeding with calculations in SCZ, we note that around r_W (or t_W) solution (3.3) can be written in the simplified form[6]

$$r_{1,2} \approx r \pm C_2 r^{\mu}, \quad \mu=\mu_2 . \tag{3.10}$$

Case (a) corresponds then to $C_2 \ll C_2^{\max}$, whereas the asymmetrical case (b) is defined by the requirement $C_2 \lesssim C_2^{\max}$.

B. The quasisymmetrical configuration solution in AZ I

Since in this case trajectories in AZ I still cluster tightly around the leading trajectories $r_1=r_2$, linearized Eq. (3.2) may be used. Further, we shall use solution (2.13) instead of that given by Eqs. (2.15) and (2.16). In the Appendix we show that by making use of the latter, more appropriate, u function, no significant change in the final result is made. So, with the help of Eq. (3.10), one has

$$r_I=\left[\frac{9}{2}\zeta\right]^{1/3} t^{2/3}+C_2\left[\frac{9}{2}\zeta\right]^{\mu/3} t^{2\mu/3}, \quad t_C<t<t_W . \tag{3.11}$$

On the other hand, both particles' motion being highly correlated in AZ I, these correlations may extend beyond u_W (i.e., after t_W) and we proceed with evaluating electrons' motion in the next zone, AZ II.

1. The solution in AZ II; $t_W < t < t_F$

We write explicitly corresponding linearized equation

$$\frac{d^2\Delta}{dt^2}=\frac{2Z\Delta}{E^{3/2}t^3} , \tag{3.12}$$

where rhs of Eq. (3.2) is treated as a small perturbation and the free-motion solution for u (i.e., for r) is substituted there

$$r^{(0)}=\sqrt{E}t . \tag{3.13}$$

We seek a solution of Eq. (3.12) in the form (quasiuniform motion)

$$\Delta=\alpha\sqrt{E}t+\delta(t) , \tag{3.14}$$

$$0<\alpha<1, \quad \delta \ll \sqrt{E}t . \tag{3.15}$$

Substituting Eq. (3.14) into Eq. (3.12) one gets

$$\frac{d^2\Delta}{dt^2}=\frac{A}{Et^2}+0\left[\frac{\delta}{\sqrt{E}t}\right] , \tag{3.16}$$

$$A=Z[\alpha(2-3\alpha)+\cdots] \tag{3.17}$$

with an approximate solution

$$\delta(t) \approx D_3'\sqrt{E}t-A\ln(\sqrt{E}t)+D_2 , \tag{3.18}$$

where D_2, D_3' are arbitrary constants. Hence, we have

$$r_{II}=\sqrt{E}t+D_3\sqrt{E}t-A\ln(\sqrt{E}t)+D_2 \tag{3.19}$$

2. Matching the solutions

In order to establish correspondence between C_2 and D_3 constants [here we do not need D_2, which is, anyway, negligibly small compared with the rest of rhs of Eq. (3.19)], we equate r_I and r_{II}, as well as their time derivatives, at $t=t_W$, which provides

$$D_3=\frac{1}{\sqrt{E}}\left[\dot{r}_1(t_W)+\frac{A}{t_W}-\sqrt{E}\right] . \tag{3.20}$$

Now, retaining only the leading terms in Eq. (3.19), one has at t_W

$$\dot{r}_1^2=\frac{4}{9}\left[\left[\frac{9\zeta}{2}\right]^{2/3} t_W^{-2/3}+2\mu C_2\left[\frac{9\zeta}{2}\right]^{1/3(1+\mu)} t_W^{2/3(\mu-2)} C_2^2\mu^2\left[\frac{9}{2}\zeta\right]^{\mu/3} t_W^{4\mu/3-2}\right]$$

$$+\frac{4A}{3t_W}\left[\left[\frac{9}{2}\zeta\right]^{1/3} t_W^{-1/3}+C_2\mu\left[\frac{9}{2}\zeta\right]^{\mu/3} t_W^{2\mu/3-1}\right]+\frac{A^2}{t_W^2} . \tag{3.21}$$

For $\dot{r}_2^2$ one has similar expression, with $C_2 \to -C_2$ [see Eq. (3.1)], so that, keeping terms linear in C_2, one obtains, through the relation (cf., Ref. 18)

$$\frac{\epsilon_1}{E-\epsilon_1}=\frac{\dot{r}_1^2}{\dot{r}_2^2} \tag{3.22}$$

the desired functional dependence of the (quasi) uniform system variable C_2 and electron 1 final energy ϵ_1

$$C_2=\frac{1}{2\mu}\left[\frac{9}{2}\zeta\right]^{1/3(1-\mu)} g^{2/3(1-\mu)}\left[\frac{2\epsilon_1}{E}-1\right]E^{\mu-1} , \tag{3.23}$$

$$g \equiv E^{3/2}t_W . \tag{3.24}$$

As can be seen, C_2 has retained its proper dependence on E [cf., Eq. (3.6)] and, which is of utmost importance here, depends linearly on ϵ_1, so that (dropping the subscript in ϵ_1)

$$\frac{dC_2}{d\epsilon}=\frac{1}{\mu}\left[\frac{9}{2}\zeta\right]^{1/3(1-\mu)} g^{2/3(1-\mu)}E^{\mu-2}=\text{const} . \tag{3.25}$$

Hence, at $\epsilon_1\approx\epsilon_2\approx E/2$ we have the uniform final-energy partition between escaping electrons. [Note that within the linear approximation C_2 is independent of A, and hence of α, cf. Eqs. (3.15) and (3.17).]

C. Asymmetrical configuration

This most unequal partition case is defined by motion within the time interval $t_W<t<t_F$, when the so-called (in case $Z=1$) monopole-dipole configuration is dominant ($r_1\ll r_2$ or vice versa). The most crucial period is (t_C,t_W), when (quasi) symmetrical configuration ($r_1\approx r_2$) develops into the other extreme.

Here, a word on the applicability of the classical picture to the situation when $\epsilon_{1,2}\ll E/2$ seems in order. As argued by Wannier,[2] the smaller the energy of an outgoing electron, the further the Coulomb zone must be pushed away from the reaction zone so as to remain "classical" (point b in Wannier division, see Fig. 1 of Ref. 2). So if Wannier's inner part of the Coulomb zone (our SCZ) is classical for $\epsilon_{1,2}\approx E/2$, it need not be for $\epsilon_{1,2}\ll E/2$. On the other hand, it is only upon entering AZ I that one of the electrons lags behind and starts losing its energy. Hence, Wannier's requirement appears automatically satisfied; the smaller the energy, the further the classical region. In other words, if the electrons are classical in SCZ, they remain such in AZ I, too. (This argument, however, does not apply to the extreme case $\epsilon_{1,2}<<<E/2$, $r=r_W$. The point $\epsilon_{1,2}\approx 0$ deserves special attention, anyway, as many numerical studies have revealed, but we dispense with considering this limiting case here.)

1. *The solution in AZ I*

We again seek an approximate solution but this time adopting a different strategy, since the electron paths are now most of the time very far away from the leading configuration. Because electron 2 is now most of the time considerably faster than the first one, it "feels," apart from an eventual Coulomb field ($Z>1$), a time-dependent dipole force of the remaining electron-ion system. On the other hand, the slower electron "sees" an essentially Coulomb attraction of the ion, perturbed by the remote electron weak repulsive force. We write Eq. (2.1) in the form

$$\frac{d^2r_2}{dt^2}\approx-\frac{Z-1}{r_2^2}-2\frac{r_1}{r_2^3},\quad r_1\ll r_2 . \tag{3.26}$$

Equation (3.26), of course, poorly describes the system at $t\gtrsim t_C$, but as time evolves, approximation improves and becomes very good at $t\lesssim t_W$. However, even with such an approximation, finding the solution of motion is an impossible task. On the other hand, since $r_2\gg 1$, we may treat rhs of Eq. (3.26) as, presumably, small perturbation (note that electron 2 is here "energetic", with $\epsilon_2\approx E$), and substitute there "zero-order" solutions for the first electron

$$r_1^{(0)}\approx\left[\frac{9}{2}\zeta_1^{\text{eff}}\right]^{1/3}t^{2/3},\quad \zeta<\zeta_1^{\text{eff}}<Z \tag{3.27}$$

where ζ_1^{eff} is an effective charge seen by the slower particle, and for the faster electron

$$r_2^{(0)}\approx\bar{v}t+R_2,\ R_2\ll\bar{v}t$$
$$\bar{v}=\vartheta\sqrt{E},\ \vartheta\le\frac{1}{2}(\sqrt{2}+\sqrt{11})=2.3654 \tag{3.28}$$

with the mean velocity $\bar{v}$. The difference between Eqs. (3.27) and (3.28) reflects the fact that while electron 1 is in AZ I, the faster particle is (mainly) in AZ II, so that a quasiuniform motion is a reasonable approximation. Equation (3.26) is solved to give

$$r_2^{(1)}\approx\frac{Z-1}{\vartheta^2E}\ln t-\frac{9Z_1}{2\vartheta^3E^{3/2}t^{1/3}}+G_1t+G_2 , \tag{3.29}$$

$$Z_1=\left[\frac{9}{2}Z\right]^{1/3} . \tag{3.30}$$

First term in Eq. (3.29) comes from the interaction with net charge of the (coupled) remaining pair, whereas the second term corresponds to the monopole-dipole interaction. By matching the solution (and its derivative) with that from Eq. (3.11), at $t=t_C$, one obtains

$$G_1=\frac{2}{3}\left[\frac{9}{2}\zeta\right]^{1/3}t_C^{-1/3}+\frac{1-Z}{\vartheta^2Et_C}-\frac{3Z_1}{2\vartheta^3E^{3/2}t_C^{4/3}}+\frac{2\mu}{3}\left[\frac{9}{2}\zeta\right]^{\mu/3}t_C^{2\mu/3-1}C_2 \tag{3.31}$$

with t_C given by Eq. (2.17). In Eq. (3.28) $\bar{v}$ is assumed to be somewhat smaller than the arithmetic mean of the initial and final velocities within AZ I.

For the slower electron, one has from Eq. (2.1)

$$\frac{d^2r_1}{dt^2}\approx\frac{Z}{r_1^2}+\frac{1}{r_2^2}\left[1-\frac{2r_1}{r_2}\right] . \tag{3.32}$$

Inserting again zero-order solutions in the rhs of Eq. (3.32), and solving the resulting (inhomogeneous) differential equation, one arrives at the "first-order" approximation:

$$r_1(t)\approx Z_1t^{2/3}-\frac{1}{\bar{v}_2^2}\ln t-\frac{9}{2}-Z_1\frac{t^{-1/3}}{\bar{v}_2^3}+B_1t+B_2 , \tag{3.33}$$

where B_1 and B_2 are arbitrary constants. Matching again solution (3.33) with Eq. (3.10) at $t=t_C$, B_1 and B_2 are determined in a similar manner

$$B_1=-\frac{2\mu}{3}Z_3^{\mu}C_2t_C^{2\mu/3-1}+\frac{2}{3}(Z_2-Z_1)t_C^{-1/3}+\frac{1}{\vartheta^2Et_C} \tag{3.34}$$

$$B_2=\left[\frac{2\mu}{3}-1\right]Z_3^{\mu}C_2t_C^{2\mu/3}+\frac{1}{3}(Z_3-Z_1)t_C^{2/3}$$
$$+\frac{1}{\vartheta^2 E}(\ln t_C-1)\ . \tag{3.35}$$

First-electron energy at $t=t_W$ is then

$$\epsilon_1=\frac{1}{2}\dot{r}_1^2(t_W)-\frac{Z}{r_1(t_W)}+\frac{1}{r_1(t_W)+r_2(t_W)}\ . \tag{3.36}$$

Neglecting the third term in Eq. (3.36), we write (second electron being practically free)

$$\frac{\epsilon_1}{E-\epsilon_1}=\frac{\dot{r}_1^2(t_W)-2Z/r_1(t_W)}{\dot{r}_2^2(t_W)}\ . \tag{3.37}$$

Substituting the corresponding expressions from Eqs. (3.29), (3.21), and (3.33)—(3.35) into Eq. (3.37), one arrives, after some lengthy but straightforward algebra, at the relation

$$C_2=F_1(Z,\vartheta)\left[F_2(Z,\vartheta)-\frac{\epsilon_1}{E}\right]E^{\mu-1}\ . \tag{3.38}$$

We omit writing the explicit dependence of the constants F_1, F_2 on Z and ϑ, because of somewhat arbitrary determination of the numerical value of the latter, which precludes a reliable comparison between Eqs. (3.23) and (3.38). However, apart from this, one can see that the relation (3.38) retains all essential features of Eq. (3.23), in particular the linear dependence of C_2 on ϵ. Hence, we conclude that in the extreme asymmetrical case one again has a random partition of the available total energy between escaping electrons.

D. Concluding remarks

To recapitulate the results from Secs. III B and III C: we have evaluated the final-energy distribution within (small) intervals

$$0<\epsilon_{1,2}<\epsilon_{1,2}^{\max}\ll\frac{E}{2}\ , \tag{3.39}$$

$$\frac{E}{2}<\epsilon_{1,2}^{\min}<\epsilon_{1,2}\lesssim E\ , \tag{3.40}$$

which appear uniform. One may estimate with a fair confidence that $\epsilon_{1,2}^{\min}\approx 4/5E$ (or, equivalently, $\epsilon_{1,2}^{\max}\approx 1/5E$) (see Ref. 18), so that both examined intervals comprise approximately 2/5 of the total energy range. As for the intermediate region,

$$\frac{E}{2}<\epsilon_{1,2}^{\max}<\epsilon_{1,2}<\epsilon_{1,2}^{\min}\ , \tag{3.41}$$

formidable mathematical difficulties preclude at present a definite conclusion from being reached, but on the basis of the present calculations it seems reasonable to believe that the region (3.41) is by no means exceptional and that a complete analysis would give an overall uniform distribution. This belief is also supported by the fact that a less elaborate calculation, with SCZ extended up to r_W (not expounded in the present work) provides for Eq. (3.38) an expression identical to that of Eq. (3.23).

IV. DISCUSSION

A. The quasiergodic hypothesis

Vinkalns and Gailitis[6] were first to evaluate numerically the final-energy distribution, calculating *$dC_2/d\epsilon$ in the free zone,* by varying C_2 values. They obtained a linear dependence of C_2 on $\epsilon_1(\epsilon_2)$ not only within the ionization interval, but somewhat outside it as well. Their rederivation of all principal Wannier's results gave a new impetus to the near-threshold studies and a series of both experimental and numerical investigations have been undertaken. In the latter a new approach has been adopted by making use of classical three-body computer codes, by which a complete scattering process is examined, by varying one of the system parameters in the initial configuration, at fixed values of the integrals of motion (E and the angular momentum L). The classical trajectories method, being completely deterministic, provides a casual link between a particular value of a single initial scattering parameter (such as a position of the atomic electron on its Kepler orbit) and C_2 value at the beginning of the evolution of the final-state configuration. All computations have shown that if an initial parameter varies uniformly within the range which corresponds to an ionization interval, so does C_2. Thus, classical trajectory method confirms Wannier's quasiergodic hypothesis, at least in the relevant part of the phase space. It is interesting to note that the original Wannier's argument rests on quite an opposite model: an almost chaotic type of motion of both electrons within the strong-interaction (quantum-mechanical) zone. That the outcomes of both deterministic (classical trajectory) and indeterministic (quantum-mechanical) models appear the same is another peculiar feature of the near-threshold ionization.

B. Classical versus quantum-mechanical model

We discuss briefly the existing controversy as for the actual mechanism of double escape near threshold. We restrict ourselves to $Z=1$ case. The classical Wannier model describes the process as continuously evolving in time and it is easy to show that within this picture, at "sufficiently small" total energy, it is the symmetrical configuration only that allows for double escape. The other interpretation[18,4] takes a quantum-mechanical point of view and regards the interaction between outgoing particles as (presumably) instantaneous exchanges of virtual photons. Final states with $\epsilon_1\approx\epsilon_2$ may be achieved via different intermediate states, however, as represented by Feynman diagrams in Fig. 2.

Now, if at $E=0$ the slower electron appears closer to the core Z, it must undergo at least one more (in addition to that already suffered in promoting the bound electron into the continuum) interaction with the other electron, so as to attain more energy from the latter. However, an ionization amplitude is a sum of all corresponding amplitudes associated with relevant diagrams in Fig. 2. Wannier classical model corresponds (but is not equivalent) to case (a), whereas Coulomb-dipole model corresponds to the second half of the process (b) (above the broken line).

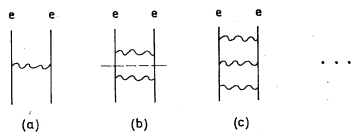

FIG. 2. Feynman diagrams for two electron final-state interactions (see text).

We shall not consider here the question whether the sum of the amplitudes for the higher-order processes, like (b), (c), etc., is competitive with that of the process (a), but note only that if it is the case, then the linear approximation, which implies angular correlations, ceases to be relevant to either of the approaches, the classical, as expounded here, and quantum-mechanical one.[18] For if the faster electron appears much further from the ion than the slower one, at the very beginning of SCZ, the less energetic particle is obliged in no way to run away in opposite direction.

A counterpart of the classical trajectory model should be a complete quantum-mechanical theory, such as *the close-coupling method,* by which higher-order effects, $a_i \to a' \to a'' \to \ldots \to a_f$, with obvious notations, are accounted for. Here, intermediate states may be both discrete and continuous ones. However, such a formidable task is still beyond our reach at present, just as is the case with the full analytical solution of the classical three-body problem.

It is interesting here to note that in the case of the model potential

$$V=-\frac{Z}{r_1^2}-\frac{Z}{r_2^2}+\frac{1}{(r_1+r_2)^2}$$

investigated by Jacobi, the energy distribution can be derived analytically,[6] and turns out to be uniform.

ACKNOWLEDGMENTS

It is our pleasure to mention useful discussion with Professor H. C. Bryant and Dr. S. Cvejanović. We would like to thank Dr. J. M. Feagin and Professor F. H. Read for sending their results prior to publication. Thanks are also due to Dr. M. Dimitrijević for drawing my attention to a number of errors in the manuscript. The work has been supported in part by Community of Science of Serbia.

APPENDIX: A MORE EXACT SOLUTION IN AZ I

We seek a solution of Eq. (3.2) without higher-order terms on rhs,

$$\frac{d^2\Delta}{dt^2}=\frac{2Z}{r^3}\Delta\ , \tag{A1}$$

with r as a given function of time, according to Eqs. (2.15), (2.16), and (2.22),

$$r=\left[\frac{9}{2}\zeta\right]^{1/3} t^{2/3}+C_3t^{4/3}+C_4t^{-1/3}\ . \tag{A2}$$

Equation (A1) can be written as

$$\frac{d^2\Delta}{dt^2}\approx\frac{2Z\Delta}{a^3t^2}\left[1-\frac{3b}{a}\left[\frac{1}{t}+ct^{2/3}\right]\right] \tag{A3}$$

with terms with C_3, C_4 as small perturbations, and with coefficients

$$a=\left[\frac{9}{2}\zeta\right]^{1/3},\ b=C_4,\ c=C_3/C_4\ . \tag{A4}$$

We assume that solution of Eq. (A3) does not differ significantly from that without the second term, and write

$$\Delta_1=t^\mu+\delta_1\equiv\Delta^{(0)}+\delta_1,\ \delta_1\ll t^\mu\ . \tag{A5}$$

Inserting the function (A5) into (A3) one obtains

$$\frac{d^2\delta_1}{dt^2}+\frac{2Z}{a^3t^2}\delta_1\approx-\frac{6Zb}{a^4t^{3-\mu}}-\frac{6bcZ}{a^4t^{4/3-\mu}}\ . \tag{A6}$$

General solution of the inhomogeneous Eq. (A6) can be easily found[22] and one has

$$\Delta_1=C_2(t^\mu+P_1t^{1-\mu}+P_2t^{\mu-1}+P_3t^{\mu+2/3})\ , \tag{A7}$$

where P_1 is an arbitrary constant and

$$P_2=-1.1833\times10^{-3}\ ZE^{-3/2}\ ,$$

$$P_3=-3.1744\times10^{-2}\ \zeta^{-5/3}ZE\ . \tag{A8}$$

To fix the idea about the magnitude of improvement introduced by additional terms in Eq. (A2), we take $Z=1$, $E=0.02$ a.u., and get

$$\Delta_1=C_2(0.968\,17+4.893\,91\times10^{-2})E^{-\mu}\ . \tag{A9}$$

The second number in the parentheses, which appears as the improvement, turns out to be about 5% of the (standard) first term.

[1]For a recent overall view of the present state of affairs see, e.g., H. Haberland, in *Proceedings of the Thirteenth International Conference on the Physics of Electronic and Atomic Collisions, Berlin, 1983, Book of Invited Lectures,* edited by J. Eichler, J. V. Hertel, and N. Stolterfoht (North-Holland, Amsterdam, 1984), pp. 711–794.

[2]G. H. Wannier, Phys. Rev. **90**, 817 (1953).

[3]See, A. Temkin in Ref. 1, p. 755, and references therein.

[4]A. Temkin, Phys. Rev. Lett. **49**, 365 (1982); also in Proceedings of the Study-Weekend on Collision Processes, Daresbury Laboratory Report No. DL/SCI/R18 (1982) (unpublished), p. 44.

[5]J. B. Donahue, P. Gram, M. Hynes, R. Hamm, C. Frost, H. C. Bryant, H. Butterfield, D. A. Clark, and W. W. Smith, Phys. Rev. Lett. **48**, 1538 (1982).

[6]J. Vinkalns and M. Gailitis, *Latvian Academy of Sciences* No. 4 (Zinatne, Riga, 1967); *Proceedings of the Fifth International Conference on the Physics of Electronic and Atomic Collisions, Leningrad, 1967,* edited by I. P. Flaks (Nauka, Leningrad, 1967), p. 648. [These authors appear first to have treated the linear configuration double escape separately, in their numeri-

cal study of the final-distribution function. Subsequently, two-dimensional configuration subspace has been used in the quantum-mechanical calculations by Peterkop and Rabik, J. Phys. B **5**, 1823 (1972), and by A. Temkin and Y. Hahn, Phys. Rev. A **9**, 708 (1974); see also footnote 3 in the last reference. Collinear motion has been treated also by Read, see Ref. 9.]

[7]P. Grujić, J. Phys. B **15**, 1913 (1982); Fizika, **15**, 213 (1983); Phys. Lett. A **96**, 233 (1983); J. Phys. B **16**, 256 (1983).

[8]See, e.g., M. S. Dimitrijević and P. V. Grujić, J. Phys. B **12**, 1837 (1979), and references therein; also cf., **16**, 297 (1983), for the case of positron-atom collisions. See, also, Ref. 9, and references therein.

[9]F. H. Read, J. Phys. B (to be published).

[10]A. R. P. Rau, J. Phys. B **9**, L283 (1976).

[11]H. Klar, J. Phys. B **14**, 3255 (1981).

[12]J. M. Feagin, J. Phys. B **17**, 2433 (1984).

[13]R. Peterkop and A. Liepinsh, J. Phys. B **14**, 4125 (1981).

[14]M. S. Yurev, Opt. Spectrosc. (USSR) **42**, 594 (1977).

[15]C. E. Bottcher, J. Phys. B **14**, L349 (1981).

[16]P. Grujić, J. Phys. B **6**, 2861 (1973).

[17]See, e.g., M. Gailitis, in Ref. 1, p. 721, and references therein.

[18]A. Temkin, J. Phys. B **7**, L450 (1974).

[19]Cf., Fig. 1 in Ref. 2, where r denotes the hyperspherical coordinate $r=\sqrt{r_1^2+r_2^2}$. Note that the present division of the configuration space is somewhat different from Wannier's in Ref. 2. Wannier Coulomb zone comprises our SCZ and AZ I.

[20]We confine ourselves to the outer-shell ionization. Otherwise, see, H. Klar, J. Phys. B **14**, 3255 (1981).

[21]As can be verified by direct inspection, usual condition at a boundary $r(\mathrm{SCZ})=r(\mathrm{AZ\,I})$, $\dot{r}(\mathrm{SCZ})=\dot{r}(\mathrm{AZ\,I})$, would yield $C_3=C_4=0$.

[22]E. Kamke, *Differentialgleichnung* (AVG, Leipzig, 1959) *(I Gewöhnliche Diff.)*.